Langmuir
Article
pubs.acs.org/Langmuir

Mixed Protein Carriers for Modulating DNA Release

M. Carmen Morán,*,† Alberto A. C. C. Pais,† Amilcar Ramalho,‡ M. Graça Miguel,† and Björn Lindman†,§

†Departamento de Química, Universidade de Coimbra, 3004-535 Coimbra, Portugal, ‡Departamento Engenharia Mecânica, Polo II, 3030 Coimbra, Portugal, and §Physical Chemistry 1, Lund University, P.O. Box 124, 22100 Lund, Sweden

Received March 26, 2009. Revised Manuscript Received June 9, 2009

Aqueous mixtures of oppositely charged polyelectrolytes undergo associative phase separation, resulting in coacervation, gelation, or precipitation. This phenomenon has been exploited in forming DNA gel particles by interfacial diffusion. We report here the formation of DNA gel particles by mixing solutions of double-stranded DNA with aqueous solutions containing two cationic proteins, lysozyme and protamine sulfate. The effect of the lysozyme/protamine ratio on the degree of DNA entrapment, surface morphology, swelling−deswelling behavior, and kinetics of DNA release has been investigated. By mixing the two proteins, we obtain particles that display higher loading efficiency and loading capacity values, in comparison to those obtained in single-protein systems. Examination of the release profiles has shown that in mixed protein particles, complex, dual-stage release kinetics is obtained. The overall release profile is dependent on the lysozyme/protamine ratio. The obtained profiles, or segments of them, are accuratelly fitted using the zero-order and first-order models, and the Weibull function. Fluorescence microscopy studies have suggested that the formation of these particles is associated with the conservation of the secondary structure of DNA. This study presents a new platform for controlled release of DNA from DNA gel particles formed by interfacial diffusion.

Introduction

Interactions between polyelectrolytes and oppositely charged amphiphiles have attracted a great deal of interest in the past two decades, because of their importance both in fundamental polymer physics and biophysics and in biological and industrial applications.[1−3] Interestingly, interactions between oppositely charged surfactants and polyelectrolytes in aqueous solutions can lead to associative phase separation, where the concentrated phase assumes the form of a viscous liquid, gel, or precipitate. This behavior has been exploited to form gel particles, which have been prepared by dropwise addition of a cellulose-based polycation solution [chitosan, *N*,*N*,*N*-trimethylammonium-derivatized hydroxyethyl cellulose (Amerchol JR-400)][4−7] to anionic [sodium dodecyl sulfate (SDS)/sodium perfluorooctanoate (FC7)] and cationic [cetyltrimethylammonium bromide (CTAB)/sodium perfluorooctanoate (FC7)][8] surfactant solutions.

Special interest has been given to particles containing DNA. By mixing solutions of DNA [either single-stranded (ssDNA) or double-stranded (dsDNA)] with solutions of the cationic surfactant, cetyltrimetrylammonium bromide (CTAB), or the protein lysozyme, researchers have formed DNA gel particles at water−water emulsion type interfaces.[9,10] The originality of this work consists of forming DNA reservoir gel particles without adding any kind of cross-linker or organic solvent. Analysis of the swelling and dissolution and DNA release responses reveals strong differences in the interaction between the surfactant and the protein with the DNA. In the CTAB−DNA particles, the formation of a physical network in which surfactant micelles form polyanionic−multicationic electrostatic complexes as cross-link points seems to play an important role in the stabilization of the DNA particles.[10]

In this work, we propose the development of biodegradable, biocompatible particles as effective drug delivery systems. These particles are formed in systems containing natural polyelectrolytes, proteins, or mixtures of proteins. Lysozyme is one of the main proteins in hen egg white, and it has an ability to cause lysis of bacterial cells.[11] Lysozyme is a globular protein that has a net charge of + 9 at neutral pH, which has been previosly used in the formation of DNA gel particles.[10] Protamines are highly positively charged (overall charge of +21), arginine-rich proteins that bind to DNA in a nonspecific manner via electrostatic interactions. Protamine sulfate adopts a random coil conformation in solution. In addition, protein protamine sulfate has been shown to condense DNA[12,13] and to deliver plasmid DNA into eukaryotic cells.[14] This property, in addition to its longtime use in pharmaceutical formulations, makes protamine a promising candidate in gene delivery formulations.

*To whom correspondence should be addressed: Departamento de Química, Universidade de Coimbra, 3004-535 Coimbra, Portugal. Telephone: +351 239 854490. Fax: +351 239 827703. E-mail: mcarmen@qui.uc.pt.

(1) Lindman, B.; Thalberg, K. In *Interactions of Surfactants with Polymers and Proteins*; Goddard, D. E., Ananthapadmanabhan, K. P., Eds.; CRC Press: Boca Raton, FL, 1993; pp 203−276.
(2) Holmberg, H.; Jönsson, B.; Kronberg, B.; Lindman, B. *Surfactants and Polymbers in Aqueous Solutions*; Wiley: West Sussex, England, 2003
(3) Dias, R. S.; Lindman, B. *DNA Interactions with Polymers and Surfactants*; Wiley-Blackwell: Hoboken, NJ, 2008.
(4) Babak, V. G.; Merkovich, E. A.; Galbraikh, L. S.; Shtykova, E. V.; Rinaudo, M. *Mendeleev Commun*. **2000**, *3*, 94–95.
(5) Julia Ferres, M. R.; Erra Serrabasa, P.; Muñoz Liron, I.; Ayats Llorens, A. Procedure for preparing capsules and for encapsulation of substances. Spain Patent ES2112150, **1998**.
(6) Lapitsky, Y.; Kaler, E. W. *Colloids Surf., A* **2004**, *250*, 179–187.
(7) Lapitsky, Y.; Eskuchen, W. J.; Kaler, E. W. *Langmuir* **2006**, *22*, 6375–6379.
(8) Lapitsky, Y.; Kaler, E. W. *Colloids Surf., A* **2006**, *282−283*, 118–128.
(9) Morán, M. C.; Miguel, M. G.; Lindman, B. *Langmuir* **2007**, *23*, 6478–6481.
(10) Morán, M. C.; Miguel, M. G.; Lindman, B. *Biomacromolecules* **2007**, *8*, 3886–3892.
(11) Ibrahim, H. R.; Higashiguchi, S.; Juneja, L. R.; Kim, M.; Yamamoto, T. *J. Agric. Food Chem*. **1996**, *44*, 1416–1423.
(12) Gaweda, S.; Morán, M. C.; Pais, A. A. C. C.; Dias, R. S.; Schillén, K.; Lindman, B.; Miguel, M. G. *J. Colloid Interface Sci*. **2008**, *323*, 75–83.
(13) Brewer, L.; Corzett, M.; Balhorn, R. *J. Biol. Chem*. **2002**, *277*, 38895–38900.
(14) Saito, G.; Amidon, G. L.; Lee, K. D. *Gene Ther*. **2003**, *10*, 72–83.

Specifically, the goal of this study is to develop and characterize DNA gel particles formed by mixing double-stranded DNA (dsDNA) with lysozyme/protamine sulfate mixtures. These particles can be used in sustained release systems as an alternative to surfactant−DNA particles.[10] The degree of DNA entrapment, the swelling−deswelling behavior, surface morphology, and DNA release kinetics are evaluated in response to the lysozyme/protamine sulfate ratio.

Materials and Methods

Materials. The sodium salt of deoxyribonucleic acid (DNA) from salmon testes with an average degree of polymerization of ~2000 base pairs (bp) was purchased from Sigma and used as received. The DNA concentrations were determined spectrophotometrically considering that for an absorbance of 1, at 260 nm, a solution of dsDNA has a concentration of 50 μg/mL.[15] All DNA concentrations are presented in molarity per phosphate group, i.e., molarity per negative charge. The ratios of absorbance at 260 and 280 nm of the stock solutions were found to be between 1.8 and 1.9, which suggested the absence of proteins.[16] Lysozyme from chicken egg white (LS), with a molecular mass of 14.3 kDa, protamine from salmon in the sulfate salt (PS), with a molecular mass of ~5.1 kDa, and Tris base were purchased from Sigma and used as received. All experiments were performed using Millipore Milli-Q deionized water (18.2 MΩ cm resistivity).

Particle Preparation. The dsDNA stock solutions were prepared in 10 mM NaBr to stabilize the DNA secondary structure in its native B-form conformation.[17,18] LS, PS, or mixtures of both were dissolved in a Tris-HCl buffer (pH 7.6). Table 1 summarizes the composition of the protein systems being studied. DNA solutions were added dropwise via a 22-gauge needle into gently agitated protein solutions (1 mL). Under optimal conditions, droplets from DNA solutions instantaneously gelled into discrete particles upon contact with the protein solution. Thereafter, the particles were equilibrated in the solutions for a period of 2 h at 25 °C. After this period, the formed particles were separated by filtration through a G2 filter and washed with 5 × 8 mL of Milli-Q water to remove the excess of salt.

Determination of the DNA Entrapment Degree. The entrapment degree was determined by quantifying both the nonbound DNA in the supernatant solution and the bound DNA in the gel particles. The entire quantity of supernatant solution containing the nonbound DNA was removed to be studied with a spectrophotometer. Thereafter, the particles were washed with Milli-Q water as described in the previous section. The particles were magnetically stirred in 10 mM Tris-HCl buffer (pH 7.6) to promote swelling and breakup of the structure. The resulting mixture, containing skins of the particles, was filtered, and the filtrates were subsequently studied by resorting to a spectrophotometer. The amount of DNA present in these skins was estimated considering the initial amount of DNA added. Loading capacity (LC) and loading efficiency (LE) were determined by

$$\text{LC}\ (\%) = [(\text{total amount of DNA} - \text{nonbound DNA})/(\text{weight of particles})] \times 100 \quad (1)$$

$$\text{LE}\ (\%) = [(\text{total amount of DNA} - \text{nonbound DNA})/(\text{total amount of DNA})] \times 100 \quad (2)$$

Table 1. Composition (w/w) of the DNA Carrier Systems

system	LS/PS (w/w)
LS	100/0
LS−PS15	85/15
LS−PS30	70/30
LS−PS50	50/50
LS−PS70	30/70
LS−PS85	15/85
PS	0/100

Three batches of particles were prepared for each system, and the results are presented as averages and standard deviations.

Swelling and Dissolution Behavior of the Particles. Studies were conducted in 10 mM Tris-HCl buffer (pH 7.6). Particles (~100 mg) were exposed to the dissolution media, at 25 °C and an agitation rate of 40 rpm using a ST 5 CAT shaking platform. At specific time intervals, the entire quantity of dissolution medium was removed and particles were placed in the container weighted. Then, a fresh dissolution medium was added. This procedure was repeated until particles were completely dissolved, or the experiment was ended (1100 h). The data were transformed into relative weight loss using

$$\text{relative weight ratio (RW)} = W_t/W_i \quad (3)$$

where W_i stands for the initial weight of the particles and W_t for the weight of the particles at time t.

Release of DNA from the Particles. Simultaneously with the studies of swelling−dissolution behavior, DNA release studies were conducted. Hence, at defined time intervals, the supernatant was collected and particles were resuspended in a fresh solution. DNA released into the supernatant solutions was quantified by measuring the absorbance at 260 nm with a spectrophotometer (Shimadzu UV-2100 UV−vis spectrophotometer).

Scanning Electron Microscopy Imaging. Scanning electron microscopy (SEM) (Philips XL30- TMP) was used to evaluate both the outer and the inner surface morphology of the particles. Previously, the particles were lyophilized overnight (−46 °C, 0.035 mbar). All the samples were kept under vacuum conditions and taken out just before the SEM observation. The dried particles were viewed without sputter coating.

Results and Discussion

Particle Preparation. Gel particles were prepared at different DNA/protein charge ratios [R = [DNA]/[P^+], where [P^+] is the protein concentration (concentrations determined per charge)]. In all cases, the DNA concentration was set to 60 mM. The choice of DNA concentration reflects the fact that it produces high-viscosity solutions, which makes it a convenient system for the preparation of stable DNA gel particles.[9,10]

The preparation of the particles was investigated at R values between 1 and 100. The formation of the DNA gel particles was initially studied using mixtures of dsDNA and LS. For low LS concentrations (R = 100), associative phase separation occurs and a two-phase region is observed (2ϕ). With an increase in the LS concentration, with R values between 10 and 1, a solid gel-like material is formed. The size of the resulting particles becomes a function of the lysozyme concentration: the higher the concentration, the smaller the observed size. However, particles swell very rapidly in water during the washing step, and their final size is around 1−2 mm.

Similar experiments were conducted using PS. For a charge ratio close to 100, associative phase separation occurs (2ϕ). With an increase in the PS concentration in the medium, and R values between 10 and 1, white, opaque particles are obtained.

On the basis of these findings, the chosen DNA/protein ratio was set to 1. Particles containing both LS and PS were prepared

(15) Sambrook, J.; Fritsch, E. F.; Maniatis, T. *Molecular Cloning: A laboratory manual*; Cold Spring Harbor Laboratory Press: Plainview, NY, 1989.
(16) Saenger, W. *Principles of Nuclei Structure*; Springer-Verlag: NewYork, 1984.
(17) Dias, R. S. DNA-Surfactants Interactions. Ph.D. Thesis, University of Coimbra, Coimbra, Portugal, **2003**.
(18) Rosa, M.; Dias, R. S.; Miguel, M. G.; Lindman, B. *Biomacromolecules* **2005**, *6*, 2164–2171.

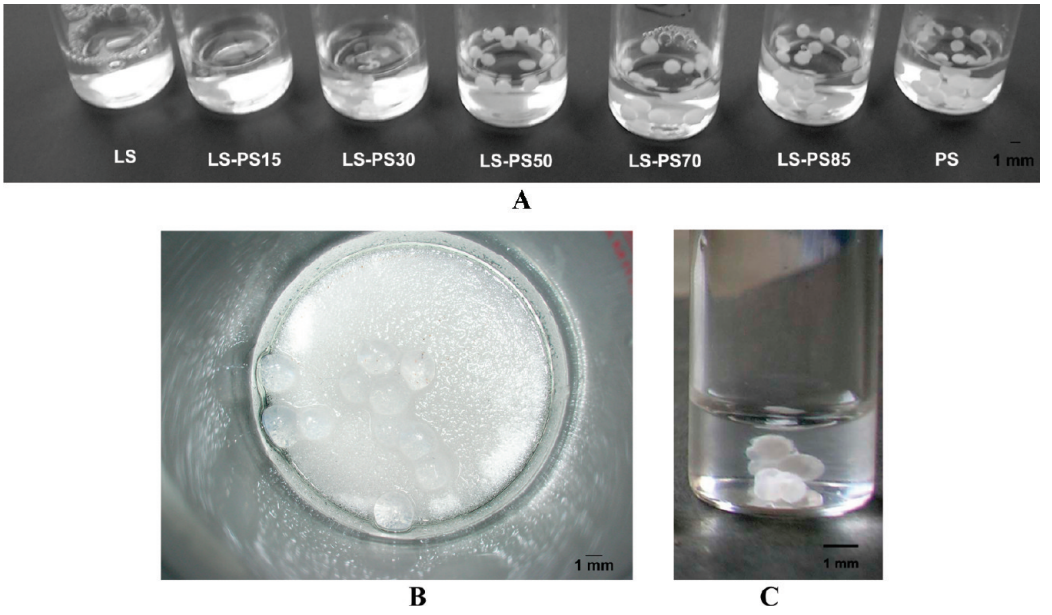

Figure 1. Representative images of the studied DNA gel particles at different LS/PS ratios, ranging from pure LS (left) to pure PS (right) (A). Detailed images of LS−DNA (B) and PS−DNA particles (C).

according to Table 1. The effect of the PS content was easily observed during the preparation process. Particles containing large amounts of PS become more visible in the solution, and opaque particles are obtained (Figure 1A). Particles obtained with only LS remain translucent after filtration (Figure 1B). In the case of particles with PS alone, they exhibit a strong tendency to aggregate (Figure 1C). Particles formed in the presence of PS exhibited a reduced size, compared with those obtained using pure LS. In the presence of PS, the diameter of the particles is ca. 1 mm.

Changes from translucent to opaque have also been observed in PNIPAAM beads[19,20] and attributed to the collapse and shrinkage of the PNIPAAM network. Using this analogy, the formation of opaque DNA particles, when the PS content is increased, probably indicates the formation of condensed structures.

Determination of the DNA Entrapment Degree. The loading efficiency (LE) values for the different systems reflect the presence of PS in the formulations. Particles containing pure LS displayed the lowest LE value (80%), compared with values of 95−100% obtained for particles containing the smaller protein (Figure 2A). Similar results were obtained in the determination of the amount of entrapped DNA as a function of the weight of the particles (LC values). The lowest LC values (0.7%) were obtained with particles formed from pure LS. Interestingly, in the presence of PS, LC values are 1 order of magnitude higher (Figure 2 B).

Significant differences were also observed in the release of DNA, once the breaking up of the particles was promoted by magnetic stirring. The values pertaining to the determination of DNA in the supernatant are summarized in Figure 2C. The observed trends can be attributed to differences in the gelation process resulting from different LS/PS ratios. Studies on surfactant and polyelectrolyte gels have shown that homogeneous gelation can give rise to homogeneous structures (solid particle), whereas a more inhomogeneous gelation process gives rise to hybrid or hollow capsules.[8] In this work, the values of complexed DNA, compared with the value of the released one, seem to confirm that the formation of solid (or condensed core) particles is favored in the presence of PS, which is also supported by visual inspection (see Figure 1A), as mentioned above.

Morphological Studies. Scanning electron microscopy imaging was conducted to establish possible differences in the morphologies for the different particles. Figure 3 shows the micrographs of the freeze-dried particles from the studied systems. The lyophilization procedure constitutes a standard protocol for the preparation of samples prior to their examination by means of SEM. Although this procedure would cause some deformation in the shape and arrangement, the PS content seems to be the most important factor for differentiating the DNA gel particles that were obtained.

LS/PS−DNA gel particles are essentially spherical (Figure 3), whereas in the case of LS−DNA particles, a not so well-defined structure has been found. This phenomenon may be attributed to the different degree of cross-linking occurring for each case. In fact, as soon as a droplet of DNA makes contact with the solution containing both proteins, peripheral cross-linking occurs immediately, preserving the almost-spherical shape of the droplet.

As shown in Figure 3, for the highest PS concentrations, particles eventually become monolithic. As a consequence of the interaction between DNA and the PS system, particles were found to quickly lose their spherical shape after the freeze-drying process.

Particle Swelling and Deswelling Kinetics. Gels are considered to have a great potential as drug reservoirs. Loaded drugs would be released by diffusion from the gels or by erosion. Hence, the release mechanism can be controlled by swelling or dissolution of the gels.[21] Figure 4 shows the relative weight ratio of the different gel particles after exposure to a buffer solution [Tris-HCl (pH 7.6)].

LS−DNA particles show a rapid and extensive weight loss which may also explain the rapid DNA release behavior of these particles as we will see below (see Figure 5). In the case of PS−DNA particles, the largest relative weight ratio was observed (RW > 5). For the high LS/PS ratio, particles absorbed an amount of water 2−3 times the initial mass (relative weight ratio, RW, of 2−3) during the swelling process. With a decrease in the LS/PS ratio, a more moderate absorption of water was observed (RW = 1−2).

(19) Park, T. G.; Choi, H. K. *Macromol. Rapid Commum.* **1998**, *19*, 167–172.
(20) Shi, J.; Alves, N. M.; Mano, J. F. *J. Biomed. Mater. Res., Part B* **2008**, *84B*, 595–603.
(21) Nam, K.; Watanabe, J.; Ishihara, K. *Eur. J. Pharm. Sci.* **2004**, *23*, 261–270.

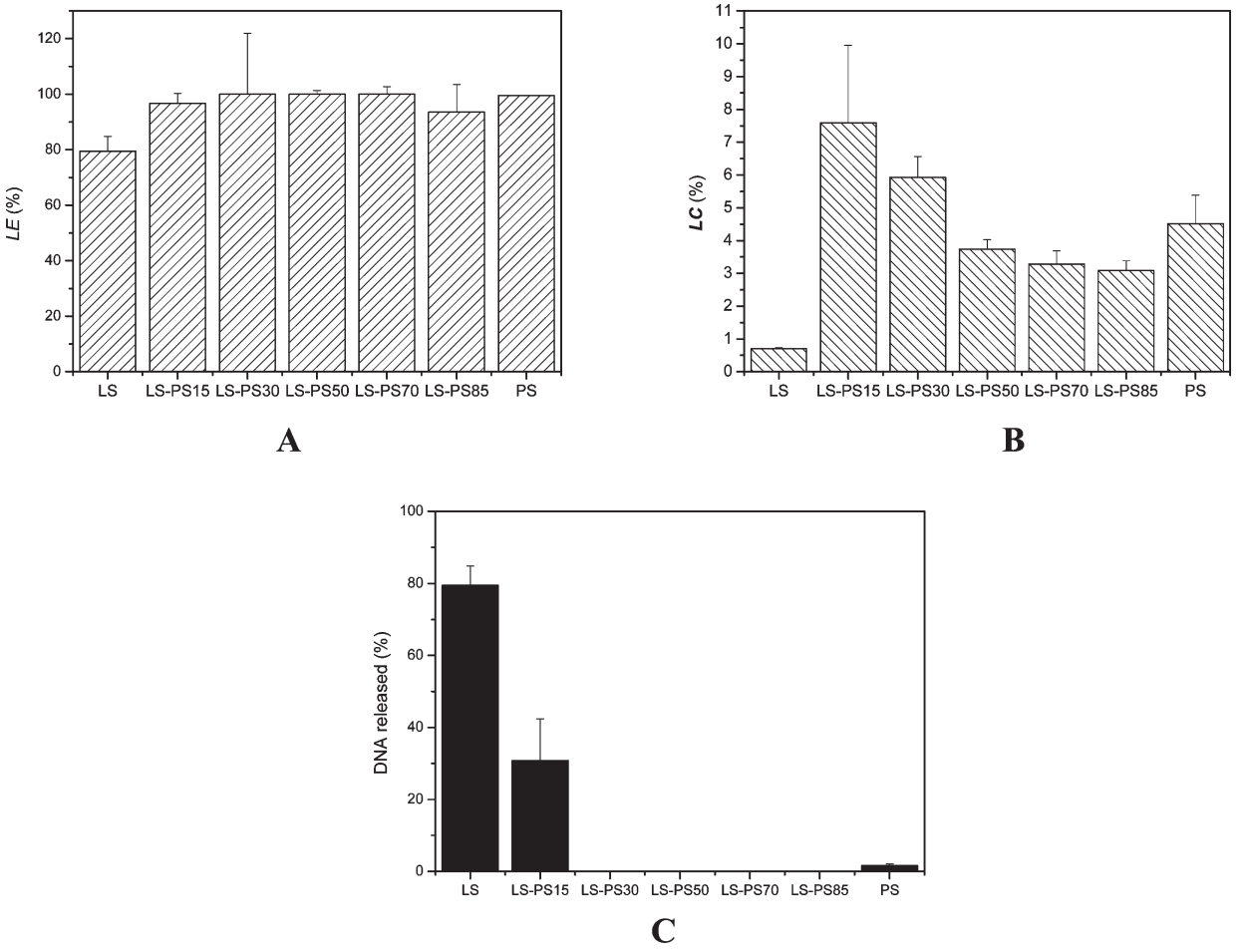

Figure 2. Characterization of the DNA gel particles with respect to the degree of DNA entrapment: (A) DNA loading efficiency (LE) and (B) loading capacity (LC). (C) Percentage of released DNA in the supernatant after particles had been magnetically stirred overnight. All values were measured in triplicate and are presented as averages and standard deviations.

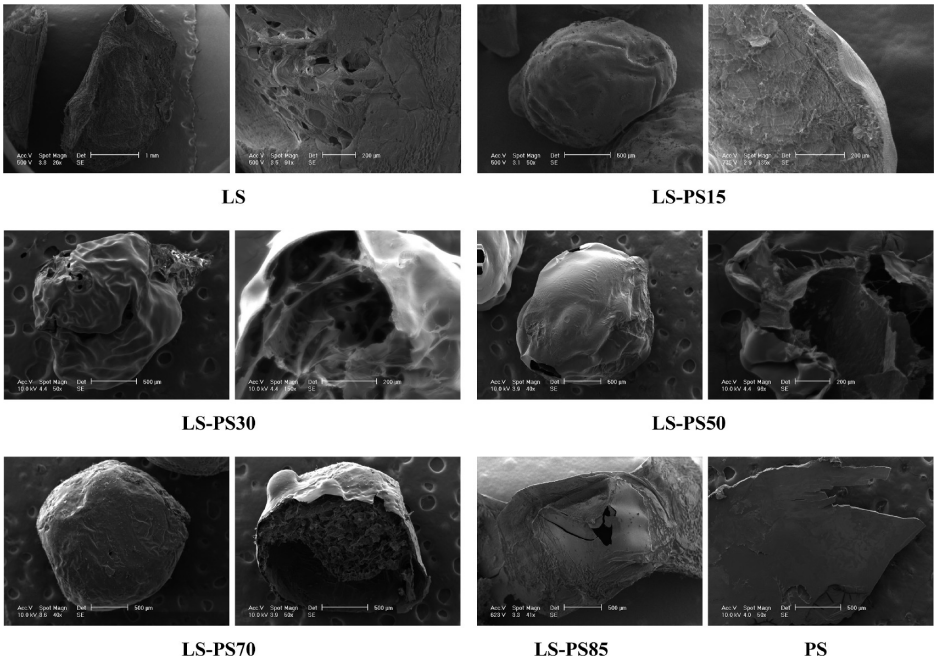

Figure 3. Scanning electron micrographs of individual particles as a function of PS content. For each formulation, the left panel corresponds to a view of the surface morphology while the right panel shows the cross section of the particle. For the LS−PS85 and PS cases, only the whole particle is shown (see the text).

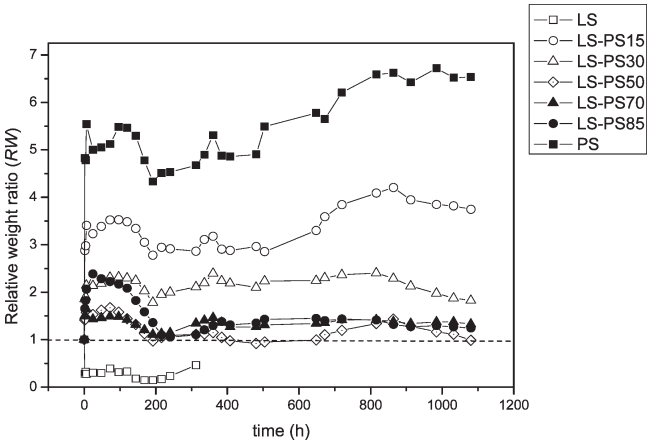

Figure 4. Time-dependent changes in the relative weight ratio for the studied DNA particles (see Table 1 for the correspondence of the acronyms).

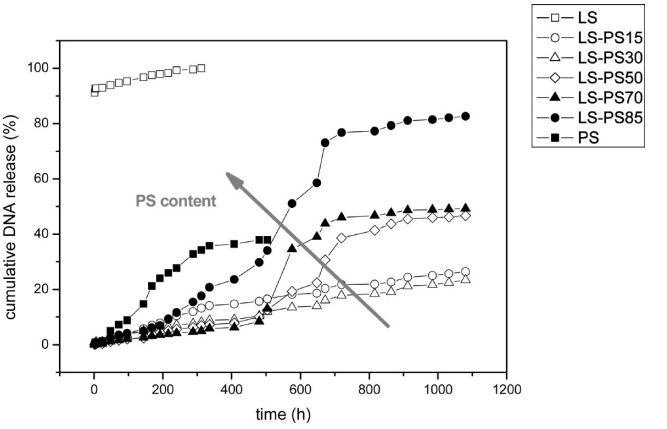

Figure 5. Time-dependent changes in DNA release profiles for the studied DNA particles (see Table 1 for the correspondence of the acronyms). The arrow was drawn as a guide for the eye.

When the particles contain PS, the swelling profiles show a common trend, in which an initial swelling is visible before the particle starts to dissolve. The initial period in the swollen state, before dissolution takes place, is independent of the PS content and lasts approximately 100 h (using the maximum of the first peak as an estimate). Then, a short time of stabilization is observed after a new, more limited maximum appears (located around 400 h). Thereafter, the RW value becomes approximately constant, with two exceptions. For PS−DNA particles, RW increases with time, while for the LS−PS15 system, a nonmonotonic behavior is observed.

Release of DNA from Particles. Particles were suspended in 10 mM Tris-HCl buffer (pH 7.6) to determine the kinetics of DNA release (see Figure 5). LS−DNA particles exhibited a fast burst release behavior by a dissolution mechanism. After 24 h, 84% of the bound DNA was released. When the formulation contains PS, the initial burst release is absent. The percentage of DNA released in the dissolution media, after 24 h, varies from 0.4 to 1.0% for protein mixed systems. The absence of a burst effect suggests that minimal amounts of unencapsulated DNA are present on the surface of the particles after formation of the particle.

For particles containing both proteins, the DNA release profiles showed slower release rates compared with those observed in the pure systems. The release rates remained almost constant in the case of particles formed at a high LS/PS ratio (LS−PS15 and LS−PS30). However, with a decrease in the LS/PS ratio, a sudden acceleration of the release was observed after ~400 h. A similar acceleration of release has been observed in HPMC/PEO hydrochlorothiazide matrices, once the liquid had saturated the core.[22] An increase in the level of absorption of water by glassy matrices, corresponding to the disappearance of the glassy core, has been found.[23] Considering these results, we can assume that a complete hydration of the core in our particles could occur after 400 h, taking into account the presence of the maximum in RW values in the swelling−dissolution experiments (Figure 4). This behavior in matrix swelling could determine the change in the rate of DNA release, which became dependent on the LS/PS ratio.

It is also noteworthy that the final release percentage is largely dependent of the LS/PS ratio. As indicated by the arrow in Figure 5, the formulations with the lower PS content release only a small percentage of the DNA present in the particles (< 20%), but this percentage increases with PS content attaining ca. 80% for the LS−PS85 formulation.

Differences in DNA gel particles prepared with LS and PS can be explained by considering both the electrostatic contribution (in terms of the number of charges and charge distribution), the conformation (globular or linear) and size of these proteins, and the differential hydrophobic contribution. While LS has a net charge of + 9 at neutral pH, PS has an overall charge of +21. In addition, LS is a globular protein, whereas PS in solution is a random coil. These proteins are characterized by significantly different molecular masses (14.3 and 5.1 kDa for LS and PS, respectively).

It is thus likely that these two molecules act complementarily upon binding to DNA. They are able to promote an increased level of charge matching and strengthened hydrophobic interaction, favored by their discrepancy in size, shape, and positioning of charges. We note that previous work from other authors[24] on sequential and simultaneous sorption of protein pairs on cation exchangers has demonstrated that the choice between competition and synergism depends on the conformation of the protein molecules.

Accordingly, when DNA gel particles are formed in mixed protein systems, PS may intercalate in the interstices formed between LS molecules. The DNA release profiles reflect the effect of PS in the mixtures. A small amount of this protein is enough to promote a significant increase in the stability of these systems (see Figure 5, LS−PS15 and LS−PS30 systems).

Evaluation of DNA Release Kinetics. The mechanism of the release of drug from swellable matrices is determined by several physicochemical phenomena. Among them, polymer water uptake, gel layer formation, and relaxation of the polymeric chains are currently regarded as being primarily involved in the modulation of drug release.[25] This is frequently addressed resorting to the Korsemeyer−Peppas model[26]

$$\frac{M_t}{M_\infty} = kt^n \tag{4}$$

in which the release exponent n is used to characterize the release mechanism. In this context, an n of 0.5 indicates Fickian release

(22) Jayan, A.; Macrae, R. J.; Walther, M.; Melia, C. D. *Pharm. Sci.* **1999**, *1*, S385.
(23) Gehrke, S. H.; Lee, P. I. In *Hydrogels for drug delivery systems*; Tyle, P., Ed.; Marcel Dekker: New York, 1990; pp 333−390.
(24) Demin, A. A.; Mogilevskaya, A. D.; Samsonov, G. V. *J. Chromatogr., A* **1997**, *760*, 105–115.
(25) Costa, P.; Lobo, J. M. S. *Eur. J. Pharm. Sci.* **2001**, *13*, 123–133.
(26) Korsmeyer, R. W.; Gurny, R.; Doelker, E.; Buri, P.; Peppas, N. A. *Int. J. Pharm.* **1983**, *15*, 25–35.

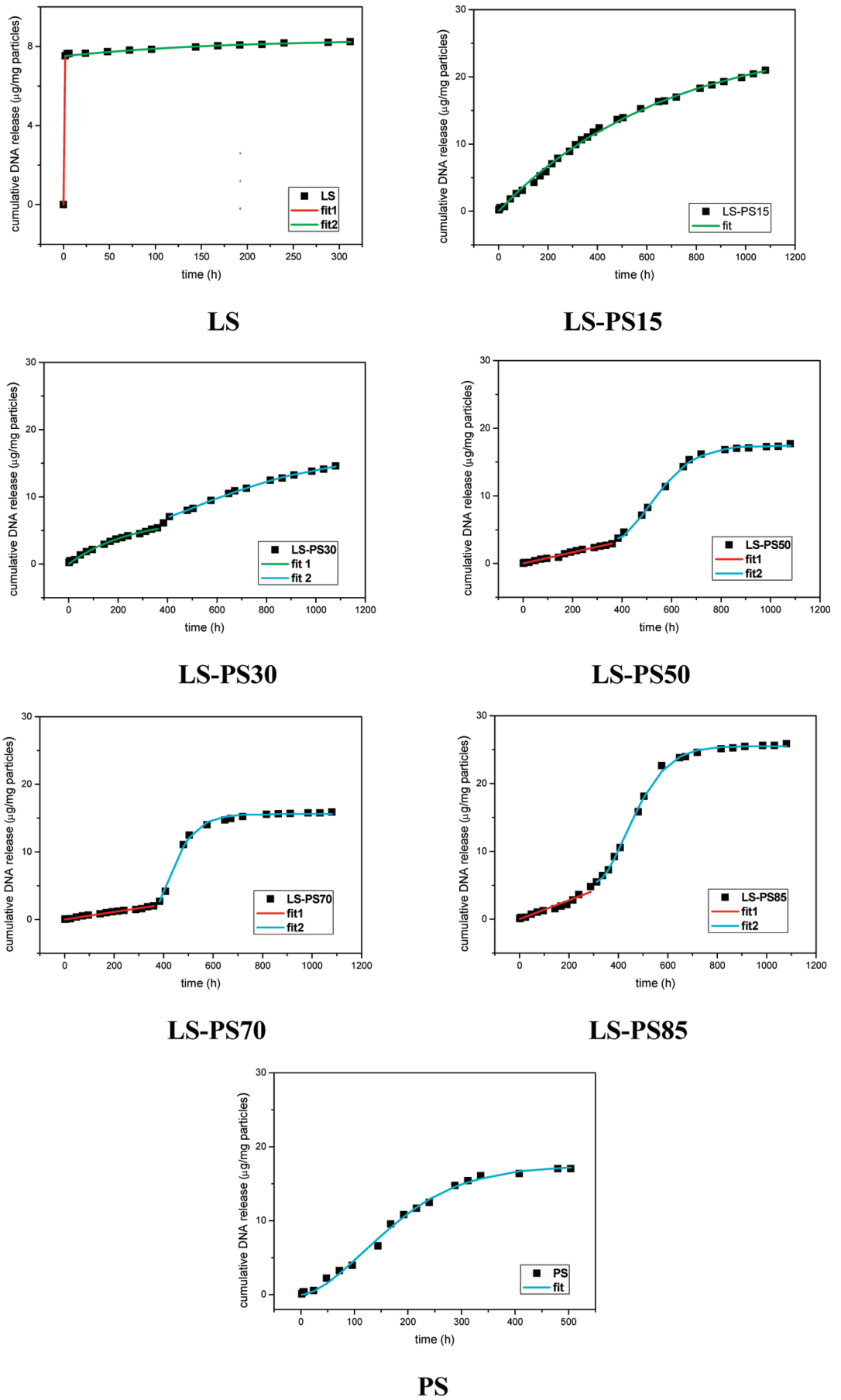

Figure 6. Experimental release profile of DNA (■) and best-fit curves for the zero-order (red line), first-order (green line), and Weibull (blue line) functions.

(diffusionally controlled release, case I) and an n of 1.0 a purely relaxation-controlled delivery which is termed case II transport. In case II diffusion, the sorption process is strongly influenced by the swelling kinetics. Intermediate values indicate an anomalous behavior (non-Fickian kinetics corresponding to coupled diffusion/polymer relaxation).[27] In some cases, n values of >1 have been observed, in a situation denoted as super case II kinetics.[28−30] In a super case II transport, there is acceleration of film sorption at longer times.[31]

Another alternative for the description of release profiles is based on the empirical use of the Weibull fuction[32]

$$M_t = M_\infty[1 - \exp(-at^b)] \quad (5)$$

where a and b are constants.

Recent studies based on Monte Carlo simulations indicate that Fickian drug release can be described by the Weibull function. These observations suggested the use of eq 5 for the analysis of the entire set of experimental data of controlled release formulations, instead of the classical analysis based on eq 4, which is usually applied for the first 60% of the release curve. Although the Weibull function has been used empirically for the analysis of release kinetics, the results obtained provide a link between the values of b and the diffusional mechanism of the release. The linear relationship established indicates not only the mathematical relevance of exponents b and n but also the physical connection of the model parameters and the release mechanism.[33]

In what follows, we use approaches based on different models that can be related to the Korsemeyer−Peppas model and the mechanistic interpretation given above. In fact, the profiles presented here, or segments of them, were accurately fitted using the zero-order (relaxation-controlled) and first-order (in which diffusion or relaxation is present) models, and the Weibull function. The latter is related, in the earlier stages, to a super case II behavior, when $b > 1$. Figure 6 shows the best fit (lines) to the experimental release profiles of DNA (squares) corresponding to the different systems.

Table 2 summarizes the model functions used in this work and the respective parameters obtained from a nonlinear least-squares fitting. Note that we have introduced one additional parameter (M_∞) into both the first-order and Weibull functions[34] to take into account the predicted asymptotic value for release, which may differ from 100%.

Let us analyze the profiles obtained in ascending order of PS content. Thus, in the case of LS−DNA particles, a zero-order equation is sufficient to describe the initial, very abrupt, burst release. Then, a first-order equation fits the later period of release, clearly indicating an increase in the importance of diffusion.

For particles containing both proteins, and the lowest PS content (LS−-PS15), a first-order model for DNA release provides an accurate least-squares fitting to the entire profile. This indicates that DNA release is dependent on the load in the matrices, and also the presence of diffusion and relaxation.

Table 2. Model Parameters Derived from the Fitting[a]

	zero-order function		first-order function					Weibull function						
	$M_t = k_0 t$		$M_t = M_0 + M_\infty\{1 - \exp[-k_1(t - t_0)]\}$					$M_t = M_0 + M_\infty\{1 - \exp[-a(t - t_0)^b]\}$						
system	k_0	r^2	M_0	t_0	M_∞	k_1	r^2	M_0	t_0	M_∞	a	b	r^2
LS	$3.76 \pm 3.60 \times 10^{-4}$	1.0	7.52	2	0.86 ± 0.11	$(5.52 \pm 1.26) \times 10^{-3}$	0.98364						
LS−PS15			0	0	26.01 ± 0.50	$1.50 \times 10^{-3} \pm 5.03 \times 10^{-5}$	0.99817						
LS−PS30			0	0	6.85 ± 0.45	$4.00 \times 10^{-3} \pm 4.56 \times 10^{-4}$	0.99601	7.05	408	9.78 ± 0.71	$2.01 \times 10^{-3} \pm 2.23 \times 10^{-4}$	$1.17 \pm 5.49 \times 10^{-2}$	0.99899
LS−PS50	$8.18 \times 10^{-3} \pm 1.26 \times 10^{-4}$	0.99114						3.73	384	13.65 ± 0.15	$4.84 \times 10^{-3} \pm 1.17 \times 10^{-4}$	$1.67 \pm 8.13 \times 10^{-2}$	0.99787
LS−PS70	$5.53 \times 10^{-3} \pm 1.05 \times 10^{-4}$	0.98942						2.69	384	12.87 ± 0.15	$1.03 \times 10^{-2} \pm 4.84 \times 10^{-4}$	1.26 ± 0.11	0.99487
LS−PS85	$1.39 \times 10^{-2} \pm 6.66 \times 10^{-4}$	0.94404						5.48	312	20.00 ± 0.16	$5.17 \times 10^{-3} \pm 1.06 \times 10^{-4}$	$1.68 \pm 6.53 \times 10^{-2}$	0.99819
PS								0	0	17.31 ± 0.37	$5.00 \times 10^{-3} \pm 1.65 \times 10^{-4}$	$1.68 \pm 9.47 \times 10^{-2}$	0.99647

[a] M_0 and t_0 represent the initial values for the released quantity and time, respectively, in fitted curves using the first-order and Weibull functions. A value different from zero in these parameters refers to a second fitted segment.

(27) Ritger, P. L.; Peppas, N. A. *J. Controlled Release* **1987**, *5*, 23–36.
(28) Ranga Rao, K. V.; Devi, P.; Buri, P. *Drug Dev. Ind. Pharm.* **1988**, *14*, 2299–2320.
(29) Ferrero, C.; Muñoz-Ruiz, A.; Jiménez-Castellano, M. R *Int. J. Pharm.* **2000**, *202*, 21–28.
(30) Munday, D. L.; Cox, P. L. *Int. J. Pharm.* **2000**, *203*, 179–192.
(31) Salamone J. C., Ed. *Polymeric materials encycopledia*; CRC Press: Boca Raton, FL, 1996; pp 2851.
(32) Langenbucher, F. *J. Pharm. Pharmacol.* **1972**, *24*, 979–981.
(33) Papadopoulou, V.; Kosmidis, K.; Vlachou, M.; Macheras, P. *Int. J. Pharm.* **2006**, *309*, 44–50.
(34) Costa, F. O.; Sousa, J. J. S.; Pais, A. A. C. C.; Formosinho, S. J. *J. Controlled Release* **2003**, *89*, 199–212.

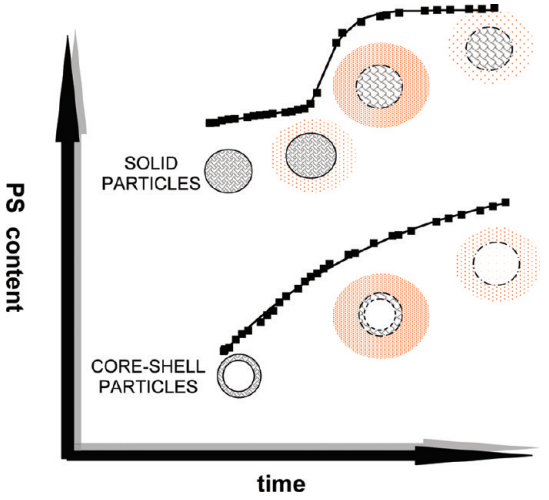

Figure 7. Schematic illustration showing the effect of composition and time on particle morphology (core−shell and solid particles), swelling, and DNA release rate on mixed protein particles. Patterns in particles represent the swelling states and the dot clouds the DNA release rate. The curves display representative DNA release profiles.

Inspection of release data corresponding to particles with a higher PS content reveals a break point (at ca. 400 h) in which the slope clearly changes to a higher value in all cases. The time point at which the second fit started is denoted as t_0 and the corresponding released quantity as M_0 (see Table 2).

The results that are listed in Table 2 suggest that the release mechanism changes during the course of the delivery. In the first stage, a zero-order equation perfectly describes the profile. The release is thus based on a pure relaxation mechanism ($n = 1$, case II). The LS−PS30 system constitutes an exception; in this case, a diffusion−relaxation combination needs to be considered, leading to the use of a first-order equation. After the break point, the fitting of the obtained profile requires models which are applicable for S-shaped profiles, such as the Weibull function. According to this model, the shape parameter (b) characterizes the curves as either exponential ($b = 1$), sigmoid, S-shaped, with upward curvature followed by a turning point ($b > 1$), or parabolic, with a higher initial slope and after that consistent with the exponential ($b < 1$). In our case, b systematically exceeds 1, originating in the sigmoidal dissolution profiles (see Table 2). Consequently, immediately after the break point, the release mechanism changes to a super case II situation and then subsequently decreases to the asymptotic value.

In the case of PS−DNA particles, a sigmoidal profile without any apparent change in mechanism is observed and we have again resorted to the Weibull model for its description. In this system, the super case II situation occurs in the earlier stages of the dissolution.

Concluding Remarks

In this work, two cationic proteins, PS and LS, were used as biocompatible carriers to form DNA gel particles by interfacial diffusion. The particles were characterized with respect to the degree of DNA entrapment, swelling and dissolution behavior, surface morphology, secondary structure of DNA in the particles, and kinetics of DNA release. Figure 7 displays schematically some of these aspects, in a perspective of composition and time evolution.

It was shown that DNA was effectively entrapped in the mixed protein solutions, protecting its secondary structure (Supporting Information). A significant increase in the degree of effective entrapment of DNA was achieved by mixing the two proteins. Direct visual and SEM observations have confirmed the difference in DNA distribution in the particles, in response to the imposed variations in protein composition. Controlling the magnitude of the DNA release and achieving controlled release systems were accomplished by changing the LS/PS ratio in the protein solution where particles were formed. Particles formed in the mixed protein system mainly showed a dual-stage release mechanism. During the first stage of the release, a zero-order profile (indicating a relaxation-controlled mechanism) was found in most cases. After this period, the release changes to a super case II mechanism, which can be ascribed to an increasing rate of matrix relaxation during drug dissolution. The beginning of this second stage is visible through an alteration in the swelling behavior. Current studies are focused on their biological properties, such as resistance to nuclease degradation and gene transfer efficiency.

Using mixtures of proteins as DNA carriers, we have obtained systems totally based on biocompatible components, with a large degree of control over the release profile. This approach will expand the usefulness of particles formed by gelation at water−water emulsion type interfaces for drug delivery applications.

Acknowledgment. This work was supported by projects from the Fundação para a Ciência e Tecnologia (FCT, POCTI/QUI/45344/2002, POCTI/QUI/58689/2004, and PTDC/QUI/67962/2006) and grants from an EU Research Training Network, CIPSNAC (Contract MRTN-CT-2003-504932) and NEONUCLEI (Contract CB/C04/2008/6).

Supporting Information Available: Data from the staining of the samples, characteristics of the fluorescence microscope device, and representative images of the secondary structure of DNA in the particles. This material is available free of charge via the Internet at http://pubs.acs.org.